Journal Pre-proof

Passivation of Black Phosphorus as Organic-phase Enzyme Platform for Bisphenol A Determination

Lidong Wu, Qingyi Meng, Zhiyuan Xu, Qiang Cao, Yushi Xiao, Huan Liu, Gang Han, Shuhua Wei

PII: S0003-2670(19)31240-1

DOI: https://doi.org/10.1016/j.aca.2019.10.030

Reference: ACA 237164

To appear in: *Analytica Chimica Acta*

Received Date: 28 August 2019

Revised Date: 14 October 2019

Accepted Date: 15 October 2019

Please cite this article as: L. Wu, Q. Meng, Z. Xu, Q. Cao, Y. Xiao, H. Liu, G. Han, S. Wei, Passivation of Black Phosphorus as Organic-phase Enzyme Platform for Bisphenol A Determination, *Analytica Chimica Acta*, https://doi.org/10.1016/j.aca.2019.10.030.

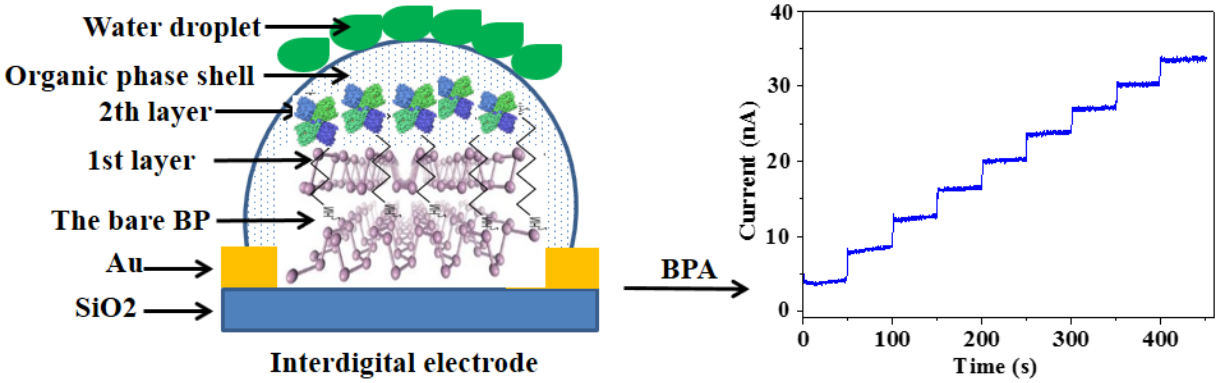

Passivation of Black Phosphorus as Organic-phase Enzyme Platform for Bisphenol A Determination

Lidong Wu[1*], Qingyi Meng[2], Zhiyuan Xu[2], Qiang Cao[1,3], Yushi Xiao[1,3], Huan Liu[1], Gang Han[1], Shuhua Wei[2]

[1.] Key Laboratory of Control of Quality and Safety for Aquatic Products, Chinese Academy of Fishery Sciences, Beijing, 100141, China

[2.] College of Information, North China University of Technology, Beijing 100043, China

[3.] College of Food Science and Technology, Shanghai Ocean University, Shanghai 201306, China

Abstract:

Black phosphorus (BP) has a high charge-carrier mobility (~1000 cm^2 V^{-1} s^{-1}), but the bare BP degrades rapidly in the presence of oxygen and water which limits the application of the BP. In this study, a simple, non-covalent passivation strategy is developed by modifying of the BP with hexamethylendiamine (HA). The functionalized BP exhibits good stability over 4 weeks. The organic phase interdigital electrode which is constructed by stable HA/BP and tyrosinase displays lowest noise signal (0.025 nA) and relatively low detection limit (10 nmol L^{-1}) for bisphenol A. This work provides a new strategy for construction of novel biofuel cell, bioelectronics and biosensors.

Keywords: Black phosphorus; Passivation; Tyrosinase; Organic phase biosensor; Interdigital electrode

Introduction:

* Corresponding author. Tel/Fax: 86-10-68690712; E-mail: lidongwu@mit.edu

Black phosphorus (BP), a layered semiconductor, has been successfully isolated in 2014 and is known as a fascinating two-dimensional (2D) material with extraordinary anisotropic mechanical, thermal, electronic and optoelectronic properties[1-4]. The intriguing properties have spurred tremendous interested in the BP. With high room-temperature mobility of 1000 $cm^2/V \cdot s$, the BP is also a promising material for electronics, optoelectronics and biosensors[5-7]. Compared to the expanding increase on the development of various kinds of BP-based electronics and optoelectronics devices, its application in biosensing is still in cradle. However, the practical applications of the BP are seriously limited due to its low stability in the presence of oxygen and water[8]. The bare BP fast transforms into PO_3^{3-} or PO_4^{3-} within 12 hours, and the degradation of the BP is most likely to start from the edges of the BP[9]. It has reported that the degradation of the BP depends on the reaction with oxygen ($P \rightarrow P_xO_y$) and water ($P_xO_y \rightarrow PO_4^{3-}$)[10, 11]. The bare BP can be completely degraded after exposed to the humid condition, which limits the applications of the BP in many research areas as field-effect transistor, light-emitting diodes, photodetectors and sensors[12, 13].

Therefore, it is necessary to build a passivation method to overcome the instability of the BP devices. Recently, various approaches have been used to protect the BP from degeneration, i.e. oxidizing top layer of the BP by oxygen plasma dry etching[14], capping of the BP with 2D graphene[15], and surface modification strategy[16, 17], etc. Among these protection methods, surface modification has proved to be one of the most effective ways to keep the chemical and electronic

properties of the BP[18, 19]. Herein, hexamethylenediamine (HA) is utilized to protect the BP from degradation. Non-covalent functionalization of the BP with HA can keep the intrinsic property of the BP through preventing oxygen approaching the surface of the BP.

The HA with diamine can serve as a bridge between the BP and enzymes. After enzyme immobilized onto the surface of the HA/BP through hydrogen bond interaction, a condensed enzyme layer is formed. Furthermore, hydrophobic organic solvent not only solves the issue that H_2O accelerates the dissolution of P_xO_y to PO_4^{3-}, but also keeps the activity of tyrosinase. Therefore, an organic-phase enzyme interdigital electrode (OPEI) has been constructed due to the high stability of the BP, high solubility of hydrophobic chemicals, and low microbial contamination. 2,5-di-tert-butyl-1,4-benzoquinone (DTBQ) (a proton-coupled electron transfer carrier) is used as the lipophilic electrolyte in chloroform to increase the sensitivity of OPEI[20, 21]. The HA/BP-based tyrosinase organic-phase interdigital electrode (BTOPI) is systematically studied by determining bisphenol A (BPA) in chloroform. To the best of our knowledge, it is the first time that the BP is used as an organic-phase enzyme biosensing platform.

2. Experimental Section

Materials and Apparatus. BPA, Bisphenol S (BPS), chloroform, dichloromethane, DTBQ and tyrosinase are obtained from Sigma Aldrich (USA). Chitosan (from crab shells, minimum 85% deacetylate) is purchased from Sigma Aldrich (USA). Phosphate buffer saline (PBS, 50mM, pH7.0) is prepared by mixing standard solution

of K_2HPO_4 and KH_2PO_4. Unless otherwise mentioned, 100 mmol L^{-1} DTBQ is used as the electrolyte in organic solvent.

Transmission electron microscopy (TEM) images are obtained by a JEOL (USA, JEM-2100). Atomic force microscopy (AFM) images obtain by peak force mode and a silicon nitride cantilever tip (Bruker). X-ray Diffraction (XRD) patterns are recorded by an X-ray diffractometer (USA, Bruker). A CHI 660B electrochemical workstation (China, CHI Instruments Inc.) is used for testing cyclic voltammetry (CV) and amperometric measurements. All the fabrication process of the interdigital electrode is completed in a super clean room to ensure the performance and the yield rates of the interdigital electrodes. Gas chromatography-mass spectrometry (GC-MS, USA, Agilent 7000 series) is used to monitor the mass of the product. BPA is added into 1 mL hexane, and analysis is performed by GC-MS using a DB-5 column (DB-5 with 0.25 μm phase, 0.25 mm i.d., 30 m). The GC-MS oven temperature is maintained at 50 °C for 3 min, and then increases to 300 °C at a rate of 40 °C/min. The oven is held at 300 °C for 10 min.

Preparation of the BP. The BP preparation process is operated in the acrylic glove box with 0.1% H_2O and O_2, which is necessary for uniform oxidation and hydroxylation of the BP surface layer. In detail, 50 mg of the bulk black phosphorus is dispersed in 100 mL chloroform and dimethylformamide (Volume:Volume; 1:1) which is bubbled with N_2 to eliminate the dissolved oxygen molecules. The mixture solution is exfoliated by ultra-sonication at 0 ^oC for 6 hours. And then, the BP is obtained in the supernatant after 6000 rpm centrifugation for 20 minutes. The BP is

immersed in a glass vial, heated up to 130^{o}C and maintained for 20 minutes. After this step, the -OH groups are formed on the surface of the BP.

Subsequently, the BP is transferred into chloroform with HA at 100 ^{o}C for 30 minutes. Through hydrogen bond interaction between the oxidized groups of the BP and NH_2 groups of HA, a stable BP with a uniform protection monolayer is formed.

Preparation of the BTOPI. The BTOPI is prepared as follows in scheme 1: 10 µL of the HA-BP solution (0.5 mg mL^{-1}) is mixed with 5 µL 10 mg mL^{-1} tyrosinase and 5 µL 1.5 mg mL^{-1} chitosan. Subsequently, the solution is shaken by vortex instrument for 30 minutes and added onto the surface of the interdigital electrode.

After incubating for 3 hours at room temperature, the surface of the interdigital electrode is dried. Then, all the electrodes are washed with 5 mL deionized water to remove the weakly binding tyrosinase before electrochemical measurements. The fabrication process of the tyrosinase organic phase interdigital electrode (TOPI) is similar with the BTOPI. The BTOPI and other interdigital electrodes are characterized by electrochemical scanning in a 5 mmol L^{-1} $[Fe(CN)_6]^{4-/3-}$ solution.

Detection of BPA by the BTOPI. BPA, which is one of the most important endocrine disrupting chemicals (EDCs), has been shown adversely influences on endocrine system of human. 10 µL BPA solution is pipetted into the chloroform (1 mL) with 0.1 mol L^{-1} DTBQ and tested by amperometric measurements under an applied potential (-0.15 V).

Safety Considerations. BPA is a EDCs agent. HA has a strong amine odor and can cause serious burns and severe irritation. Material safety data sheet (MSDS)

information for these chemicals must be consulted, and precautions need to be taken for handling them (i.e., wearing gloves, eyeglasses and mask).

3. Results and Discussion

The bare BP degrades in 1 minute under strong electronic beam from TEM and SEM images, thus their images are not caught by TEM. After coating with HA, the BP becomes stable and can stand strong electronic beam over 30 minutes. The structure and morphology of the HA/BP are characterized by TEM, SEM and AFM. Figure 1A shows that the high-quality HA/BP with lattice fringes has been obtained through liquid-exfoliated method. The selected area diffraction pattern of the HA/BP (Figure 1B) displays the orthorhombic crystalline character of the HA/BP.

The stability of the HA/BP is characterized by AFM. As shown in Figure 2A and B, without coating HA, most of the BP has been degraded by oxygen in aqueous solution after 12 hours. As soon as the bare BP is exposed to oxygen, it reacts with O_2 and forms an inevitable phosphorus oxide layer ($P_4 + 5O_2 \rightarrow P_4O_{10}$). The oxidized BP interacts with H_2O and turns into phosphoric acid by the following reaction ($P_4O_{10} + 6H_2O \rightarrow 4H_3PO_4$)[12]. Thus, it appears as ambiguous morphology on the BP edges, as shown in Figure 2B. After HA coating on the surface of the BP, the HA/BP becomes stable and keeps its original form in aqueous solution over 4 weeks (Figure 2C and D). The main reason is that a phosphorus oxide layer is formed on the surface of the BP after exposing under O_2. The phosphorus oxide layer interacts with HA through hydrogen bond interaction, and the HA layer protects the BP from H_2O reaction. The thickness of HA coating on the BP is characterized by AFM. As shown

in Figure 2E, the thickness of HA is approximately 1.4 nm (a uniform HA layer is formed). Furthermore, the tyrosinase anchors on the surface of the HA/BP through hydrogen-bond interaction. A uniform layer is formed on the surface of the HA/BP, and its thickness is around 11 nm. It is consistent with three dimensions of tyrosinase[22]. Furthermore, the structural information of the BP is also characterized by XRD. As shown in Figure 2F, XRD pattern of the BP also shows the orthorhombic crystal structure along the (040) direction. After coating with HA, the XRD pattern of the HA/BP does not change (data does not show in Figure 2F). This confirms that the HA/BP keeps its original form.

As is well-known, biosensing materials play a key role in the performances of biosensors. The BP has become one of the brightest stars among 2-dimensional materials after its first mechanical exfoliation from bulk BP in 2014. The BP shows excellent performances as electronic or optoelectronic devices, sensors, etc. However, there is few researches using the BP as a biosensing platform, even the charge carrier of the BP is as high as 1000 $cm^2/V \cdot s$. This is mainly due to its easy degeneration in aqueous solution. After the stable BP is obtained in this work, it will explore more promising applications. In this study, the modification process of the interdigital electrode is monitored by CV in a $[Fe(CN)_6]^{4-/3-}$ solution. Figure S1 shows the CV signals of the interdigital electrode, TOPI and BTOPI (curve a, curve b and curve c) in a 5 mmol L^{-1} $[Fe(CN)_6]^{4-/3-}$ solution. Compared to the interdigital electrode, the response signal of the TOPI (curve b) decreases remarkably in $[Fe(CN)_6]^{4-/3-}$ solution. This is primarily due to the low-conductivity tyrosinase covering the surface of

interdigital electrode. After the HA/BP and the tyrosinase immobilizes onto the interdigital electrode, the response signal increases significantly. This is mainly due to the high-conductivity HA/BP improving the electron transfer rate between ($[Fe(CN)_6]^{4-/3-}$) and the interdigital electrode. The results indicate that the tyrosinase/HA/BP composite is successfully immobilized on the interdigital electrode.

The tyrosinase/HA/BP is used to construct an organic phase interdigital electrode for monitoring the hydrophobic BPA. BPA, one of the highest volume industrial chemicals, is banned in the United States for using in baby bottles due to its reproductive and developmental toxicity[23]. It is readily soluble in organic solvent but has poor solubility in water[24]. For example, it is over an order of magnitude more soluble in chloroform than in aqueous solution[25-27]. Thus, BPA can rapidly transfer from aqueous solution to organic solution (liquid-liquid extraction). Based on the above reasons, BPA is monitored by the BTOPI in chloroform. The solubility of BPA in chloroform is over an order of magnitude than in water[28], with an extra benefit being 40-fold higher solubility than in water of the co-substrate oxygen.

The operating potential of the BTOPI is checked in Figure S2. The response signal increases rapidly as the potential decreases from 0 to -0.2 V. In order to get good signal-to-noise (S/N) characteristics, -0.15 V is selected as the applied potential. Such a low potential can minimize potential interferences from electroactive species. Figure 3A displays the amperometric response (at -0.15V) of the BTOPI (curve a), the TOPI (curve b) and the bare interdigital electrode (curve c) to the successive addition of BPA under constant stirring. The BP modified interdigital electrode without tyrosinase

does not response to BPA. While the TOPI and the BTOPI have obvious amperometric signals with the additions of 0.1 μmol L^{-1} BPA, reaching 95% of steady state current within 5 seconds. Such a rapid response of the BTOPI could be attributed to the fast diffusion of BPA from organic solvent to the immobilized tyrosinase. Figure 3B shows the calibration curves of the response signals of these biosensors versus BPA concentrations (from 100 nmol L^{-1} to 1 μmol L^{-1}). It indicates that the BTOPI exhibits higher response signals than the TOPI due to the high-conductivity BP. The sensitivity of the BTOPI is 0.26 μA μmol^{-1} cm^{-2}, which is above 10 times higher than that of TOPI (0.018 μA μmol^{-1} cm^{-2}). The linear range of the BTOPI is from 5×10^{-8} to 1×10^{-6} mol L^{-1} with a correlation coefficient of 0.9993. The noise signal is stable and approximately 2.5×10^{-11} A, and its detection limit is 10 nmol L^{-1}.

The analytical performances of the BTOPI have been compared with other tyrosinase biosensors (Table 1). From table 1, it shows that the noise of the BTOPI is the lowest among all the biosensors. The reason is that the low stability of product (*o*-quinones) in aqueous solution is rapidly polymerized to polyaromatic pigments. The pigments inactivate the tyrosinase and limit the substrate and product transferring from the solution to the catalyst center of the tyrosinase. As a result, the background noise signals of the biosensors in aqueous solution increase very fast with the continuous reaction. However, BPA can be quantitatively converted to stable *o*-quinones without further polymerization in organic solvent. This causes low background noise signal. The stable *o*-quinones is verified by GC-MS (Figure S3). Based on the above reasons, the detection limit of the BTOPI is lowest among these

biosensors even its sensitivity is not the highest among them. The results indicate that this biosensor is an excellent candidate for the detection of BPA.

Reproducibility is another attractive feature of the BTOPI. 0.1 μmol L^{-1} BPA is detected by the BTOPI for 8 repeated measurements, and the results show highly reproducible amperometric peaks with a relative standard deviation (RSD) of 0.5% (Figure 3C). This indicates that the fabrication reproducibility is acceptable. Furthermore, the long-term stability of the BTOPI in chloroform is investigated by 8 consecutive measurements for 0.1 μmol L^{-1} BPA within 8 months. When the BTOPI is not in use, it is saturated in chloroform and stored in the refrigerator at 4 ^{o}C. It retains over 65% of its initial current response even after 180 days storage.

The good sensing performances of the BTOPI may be attributed to the following factors: the large surface area of the BP could greatly increase the active surface area of the interdigital electrode; the high conductivity of the BP could improve the electron transfer rate between the interdigital electrode and BPA in organic solvent; the layer-by-layer architectures could provide a broad space for the easy transfer route of BPA through organic solvent to the immobilized tyrosinase (shown in Scheme 2A), and DTBQ as new electrolyte could enlarge the signal of the BTOPI (the mechanism is shown in Scheme 2B). As shown in Scheme 2, the tyrosinase catalyzes two distinct oxidation reactions. In step 1, the tyrosinase accomplishes the oxidation of monophenol to diphenols by oxygen. In step 2, o-diphenols are oxidized to the formation of o-quinones. The o-quinones spontaneously reduce by DTBQ. Thus, the tyrosinase and DTBQ work together to enlarge the signal of the BTOPI.

In addition, the BTOPI is used to determine BPA leaching from plastic oil containers and oyster sauce containers which are purchased from a local supermarket. These plastic containers are heated up by microwave instrument for 30 minutes and then transfer 10 μL extracted oil into 1 mL chloroform. The oil samples are analyzed by this biosensor with amperometric measurements. The results show that none of them exists BPA. It indicates that most of the PC containers have been replaced by other plastic containers. When 100 nmol L^{-1} BPA is spiked into the analytical samples during sample preparation, the recovery values of the samples are above 85% for the 100 nmol L^{-1} level. Overall, this method is a potential approach for BPA test due to its acceptable recovery. Furthermore, four water samples from aquaculture are extracted by chloroform, and tested by the BTOPI. The amperometric results show that only one sample exists 350 nmol L^{-1} BPA. The other potential co-existing plasticizer interferences and derivatives (i.e. BPS) are checked by this biosensor (Figure S4). There is no response signal because they are not the substrate of tyrosinase. It reveals that this biosensor is a potential and efficient tool for the selective determination of BPA from coexisting chemicals.

4. Conclusion

In this study, the BP has been successfully modified by HA which has two amine groups. The HA/BP can anchor tyrosinase through hydrogen-bond interaction. Furthermore, as the battery related field explosive growth, more and more lipophilic electrolytes will accelerate the development of organic phase biosensor. It also suggests that the HA/BP hybrid not only function as a good electrical conductor but

also serve as a stable enzyme-based platform in organic solvent. Thus, the HA/BP is a promising building blocks for biosensors and bioelectronics.

Acknowledgment

This work was supported by Central Public-interest Scientific Institution Basal Research Fund, CAFS (NO. 2019ZD08), the National Natural Science Foundation of China (No. 21307161), and NSFC-RFBR international cooperation and exchange program (NSFC grant No.81811530114, RFBR grant No. 185253017). Author would like to thank Prof. Alexander M. Klibanov (Chemistry Department, MIT) who give me lots of suggestion in experiment details.

References

[1] J.R. Brent, N. Savjani, E.A. Lewis, S.J. Haigh, D.J. Lewis, P. O'Brien, Production of few-layer phosphorene by liquid exfoliation of black phosphorus, Chem Commun, 50 (2014) 13338-13341.

[2] Z.Q. Zhao, H. Yin, K. Cai, W.Q. Zhou, Mechanical stability of a nanotube from monolayer black phosphorus with the [110] direction as the tube's circumference or generatrix, Phys Chem Chem Phys, 20 (2018) 3465-3473.

[3] L.K. Li, Y.J. Yu, G.J. Ye, Q.Q. Ge, X.D. Ou, H. Wu, D.L. Feng, X.H. Chen, Y.B. Zhang, Black phosphorus field-effect transistors, Nat Nanotechnol, 9 (2014) 372-377.

[4] Q. Li, Q. Zhou, X. Niu, Y. Zhao, Q. Chen, J. Wang, Covalent Functionalization of Black Phosphorus from First-Principles, The journal of physical chemistry letters, 7 (2016) 4540-4546.

[5] J.S. Qiao, X.H. Kong, Z.X. Hu, F. Yang, W. Ji, High-mobility transport anisotropy and linear dichroism in few-layer black phosphorus, Nat Commun, 5 (2014) 4475-4482.

[6] Y. Li, S.X. Yang, J.B. Li, Modulation of the Electronic Properties of Ultrathin Black Phosphorus by Strain and Electrical Field, J Phys Chem C, 118 (2014) 23970-23976.

[7] M. Engel, M. Steiner, P. Avouris, Black Phosphorus Photodetector for Multispectral, High-Resolution Imaging, Nano Lett, 14 (2014) 6414-6417.

[8] G. Lee, S. Kim, S. Jung, S. Jang, J. Kim, Suspended black phosphorus nanosheet gas sensors, Sensor Actuat B-Chem, 250 (2017) 569-573.

[9] Y.T. Chen, R. Ren, H.H. Pu, J.B. Chang, S. Mao, J.H. Chen, Field-effect transistor biosensors with two-dimensional black phosphorus nanosheets, Biosens Bioelectron, 89 (2017) 505-510.

[10] C.J. An, Y.H. Kang, C. Lee, S.Y. Cho, Preparation of Highly Stable Black Phosphorus by Gold Decoration for High-Performance Thermoelectric Generators, Adv Funct Mater, 28 (2018) 1800532-1800539.

[11] D.H. Kwak, H.S. Ra, J. Yang, M.H. Jeong, A.Y. Lee, W. Lee, J.Y. Hwang, J.H. Lee, J.S. Lee, Recovery Mechanism of Degraded Black Phosphorus Field-Effect Transistors by 1,2-Ethanedithiol Chemistry and Extended Device Stability, Small, 14 (2018) 1703194-1703201.

[12] C.C. Mayorga-Martinez, Z. Sofer, M. Pumera, Layered Black Phosphorus as a Selective Vapor Sensor, Angew Chem Int Edit, 54 (2015) 14317-14320.

[13] P. Li, D.Z. Zhang, C.X. Jiang, X.Q. Zong, Y.H. Cao, Ultra-sensitive suspended atomically thin-layered black phosphorus mercury sensors, Biosens Bioelectron, 98 (2017) 68-75.

[14] B.S. Wan, Q.H. Zhou, J.Y. Zhang, Y. Wang, B.C. Yang, W.M. Lv, B.S. Zhang, Z.M. Zeng, Q. Chen, J.L. Wang, W.H. Wang, F.S. Wen, J.Y. Xiang, B. Xu, Z.S. Zhao, Y.J. Tian, Z.Y. Liu, Enhanced Stability of Black Phosphorus Field-Effect Transistors via Hydrogen Treatment, Adv Electron Mater, 4 (2018) 1700455-1700462.

[15] C.Y. Xing, G.H. Jing, X. Liang, M. Qiu, Z.J. Li, R. Cao, X.J. Li, D.Y. Fan, H. Zhang, Graphene oxide/black phosphorus nanoflake aerogels with robust thermo-stability and significantly enhanced photothermal properties in air, Nanoscale, 9 (2017) 8096-8101.

[16] F. Telesio, E. Passaglia, F. Cicogna, F. Costantino, M. Serrano-Ruiz, M. Peruzzini, S. Heun, Hybrid nanocomposites of 2D black phosphorus nanosheets encapsulated in PMMA polymer material: new platforms for advanced device fabrication,

Nanotechnology, 29 (2018)295601-295609.

[17] X.W. Gao, Y.H. Chen, L. Johnson, P.G. Bruce, Promoting solution phase discharge in Li-O-2 batteries containing weakly solvating electrolyte solutions (vol 15, pg 882, 2016), Nat Mater, 15 (2016) 882-888.

[18] W.L. Guo, H.Z. Song, S.C. Yan, Stable black phosphorus quantum dots for alkali PH sensor, Opt Commun, 406 (2018) 91-94.

[19] J.D. Wood, S.A. Wells, D. Jariwala, K.S. Chen, E. Cho, V.K. Sangwan, X.L. Liu, L.J. Lauhon, T.J. Marks, M.C. Hersam, Effective Passivation of Exfoliated Black Phosphorus Transistors against Ambient Degradation, Nano Lett, 14 (2014) 6964-6970.

[20] X.W. Gao, Y.H. Chen, L. Johnson, P.G. Bruce, Promoting solution phase discharge in Li-O-2 batteries containing weakly solvating electrolyte solutions, Nat Mater, 15 (2016) 882-888.

[21] J.H. Yu, H.X. Ju, Pure organic phase phenol biosensor based on tyrosinase entrapped in a vapor deposited titania sol-gel membrane, Electroanal, 16 (2004) 1305-1310.

[22] M.G. Bridelli, Self-assembly of melanin studied by laser light scattering, Biophysical chemistry, 73 (1998) 227-239.

[23] K.K. Reza, M.A. Ali, S. Srivastava, V.V. Agrawal, A.M. Biradar, Tyrosinase conjugated reduced graphene oxide based biointerface for bisphenol A sensor, Biosens Bioelectron, 74 (2015) 644-651.

[24] C. Nicolucci, S. Rossi, C. Menale, T. Godjevargova, Y. Ivanov, M. Bianco, L. Mita, U. Bencivenga, D.G. Mita, N. Diano, Biodegradation of bisphenols with immobilized laccase or tyrosinase on polyacrylonitrile beads, Biodegradation, 22 (2011) 673-683.

[25] R. Battino, T.R. Rettich, T. Tominaga, The Solubility of Oxygen and Ozone in Liquids, J Phys Chem Ref Data, 12 (1983) 163-178.

[26] T. Sato, Y. Hamada, M. Sumikawa, S. Araki, H. Yamamoto, Solubility of Oxygen in Organic Solvents and Calculation of the Hansen Solubility Parameters of Oxygen, Ind Eng Chem Res, 53 (2014) 19331-19337.

[27] J. Corrales, L.A. Kristofco, W.B. Steele, B.S. Yates, C.S. Breed, E.S. Williams, B.W. Brooks, Global Assessment of Bisphenol A in the Environment: Review and Analysis of Its Occurrence and Bioaccumulation, Dose-Response, 13 (2015) 1-29.

[28] S.Y. Okazaki, J. Michizoe, M. Goto, S. Furusaki, H. Wariishi, H. Tanaka, Oxidation of bisphenol A catalyzed by laccase hosted in reversed micelles in organic media, Enzyme Microb Tech, 31 (2002) 227-232.

[29] L. Wu, D. Deng, J. Jin, X. Lu, J. Chen, Nanographene-based tyrosinase biosensor for rapid detection of bisphenol A, Biosens Bioelectron, 35 (2012) 193-199.

[30] M. Portaccio, D. Di Tuoro, F. Arduini, M. Lepore, D.G. Mita, N. Diano, L. Mita, D. Moscone, A thionine-modified carbon paste amperometric biosensor for catechol and bisphenol A determination, Biosens Bioelectron, 25 (2010) 2003-2008.

[31] H. Yin, Y. Zhou, J. Xu, S. Ai, L. Cui, L. Zhu, Amperometric biosensor based on tyrosinase immobilized onto multiwalled carbon nanotubes-cobalt phthalocyanine-silk fibroin film and its application to determine bisphenol A, Anal Chim Acta, 659 (2010) 144-150.

[32] X. Lu, X. Wang, L. Wu, L. Wu, Dhanjai, L. Fu, Y. Gao, J. Chen, Response Characteristics of Bisphenols on a Metal-Organic Framework-Based Tyrosinase Nanosensor, ACS Appl Mater Interfaces, 8 (2016) 16533-16539.

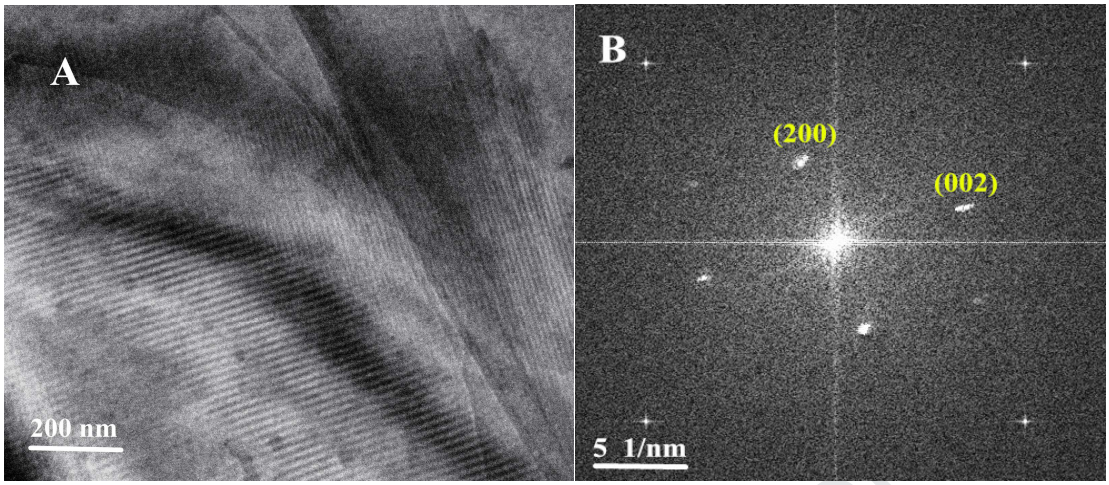

Figure 1. (A) TEM image of the HA/BP and (B) selected area electron diffraction pattern of the HA/BP under high-magnification condition.

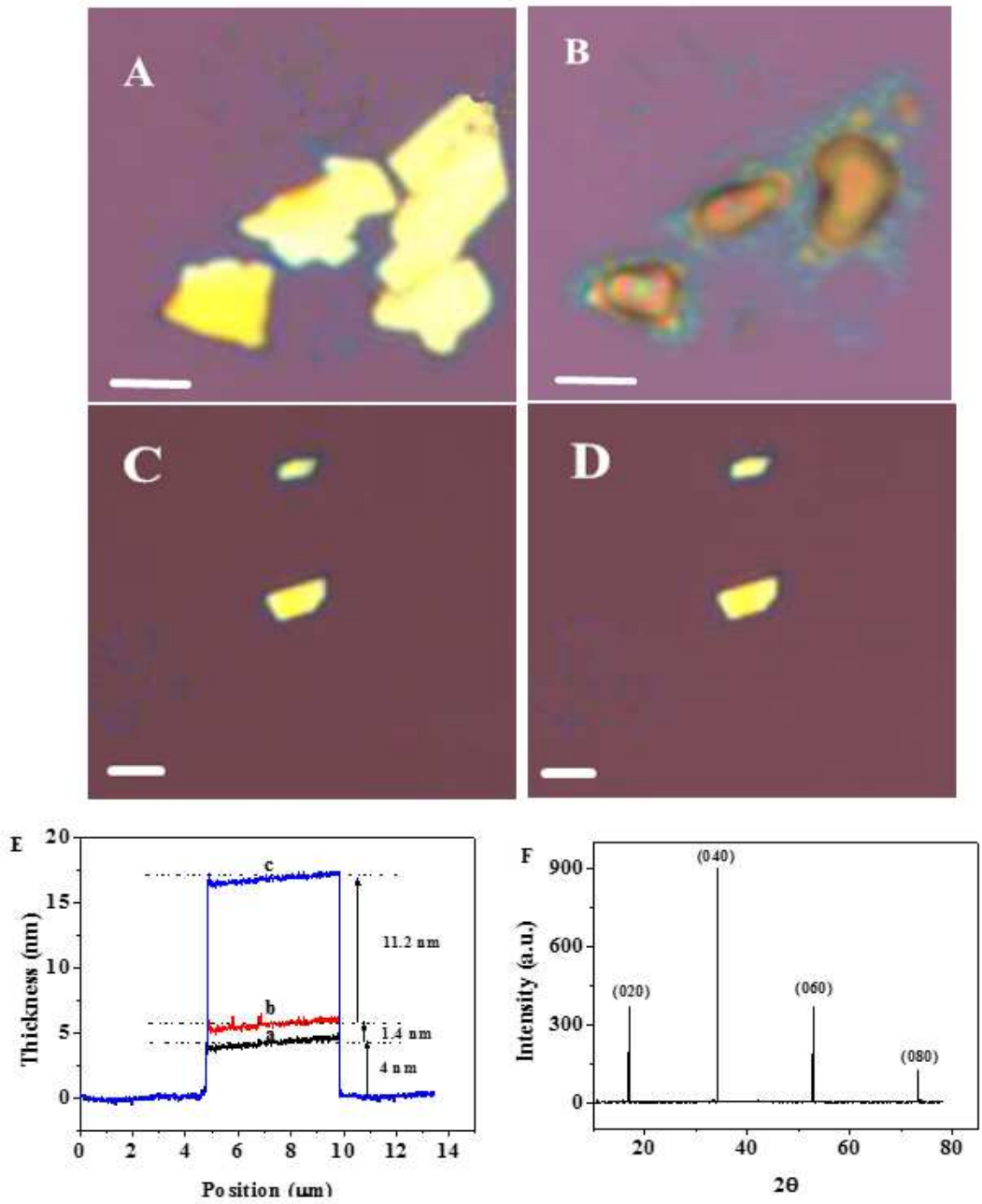

Figure 2. Atomic force microscopy images of (A) the bare BP, (B) the bare BP in water for 12 hours, (C) the HA/BP and (D) the HA/BP in water for 4 weeks, the white bar is 10 µm. (E) The AFM characterization of the thickness of the same BP before and after coating protection layer, with the locations of height profile marked by dotted lines, and (F) The XRD pattern of the BP.

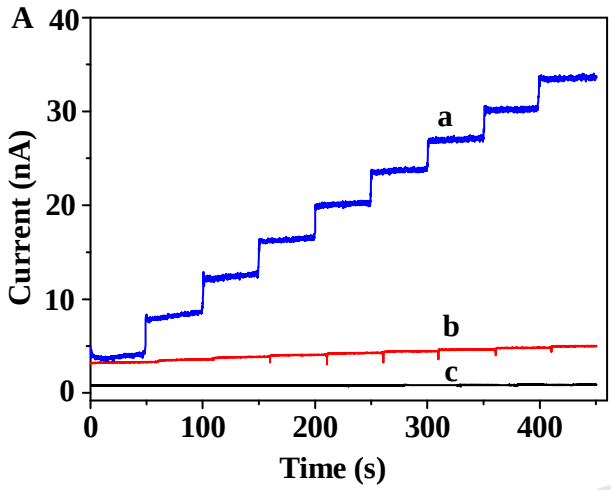

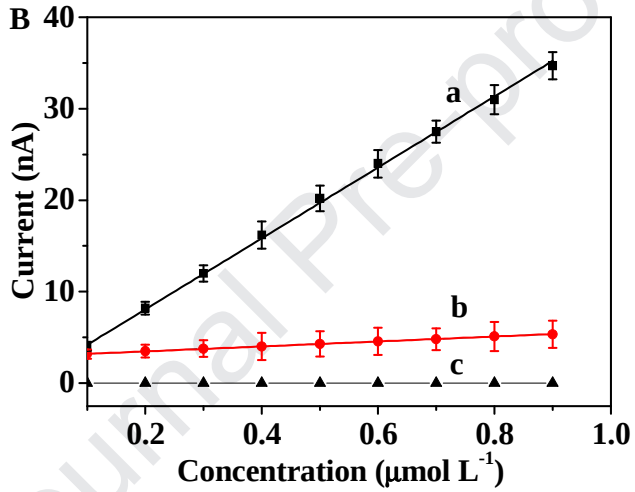

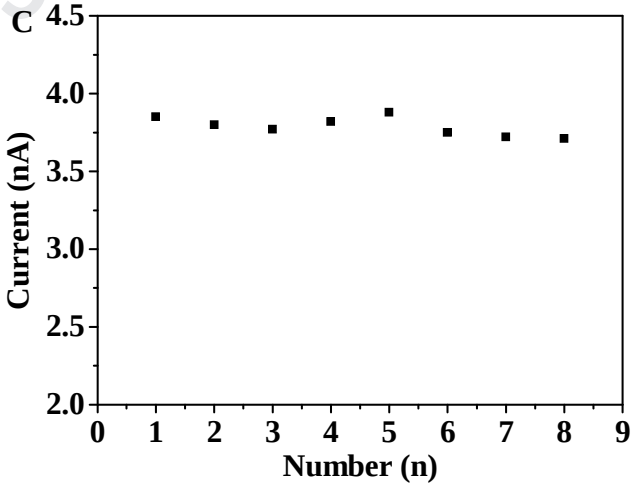

Figure 3. (A) Amperometric measurement of the BTOPI (a), the TOPI (b) and the bare interdigital electrode (c) with successive addition of 10 μL 10 μmol L^{-1} BPA into 1

mL chloroform solvent. Applied potential: -0.15 V versus Ag/AgCl. (B) The corresponding calibration curves of steady-state currents versus concentrations of BPA. The standard deviations are all less than 5%. (C) The stability of 8 repeated measurements for 10 μL 10 μmol L^{-1} BPA into 1 mL chloroform with 0.1 M DTBQ as electrolytes.

Table 1. Comparison of analytical performances of the BTOPI with other tyrosinase biosensor for detection of BPA.

Modified biosensor	Linear range (μM)	Sensitivity (μA μmol^{-1} cm^{-2})	Detection limit (nM)	Background noise (nA)	Reference
BTOPI	0.05-1.0	0.26	10.0	0.025	Present work
NGP-Tyr-Chi/GC	0.1-2.0	3.11	33.0	0.2	[29]
Thionine-Tyr/CP	0.15-45.0	1.21	150.0	2.0	[30]
MWNT-SF-Tyr/GC	0.05-3.0	0.17	30.0	1.0	[31]
CuMOF-Tyr/GC	0.05-3.0	4.48	13.0	10.0	[32]

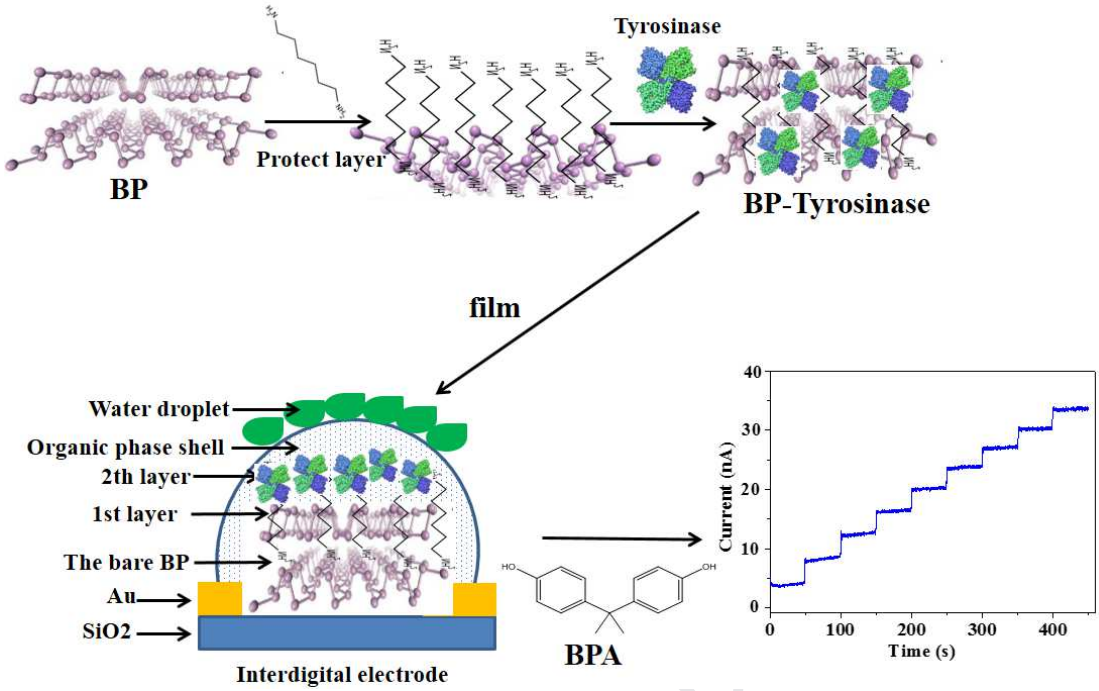

Scheme 1. Schematic diagram of the fabrication process and detection mechanism of the BTOPI for BPA in organic solvent.

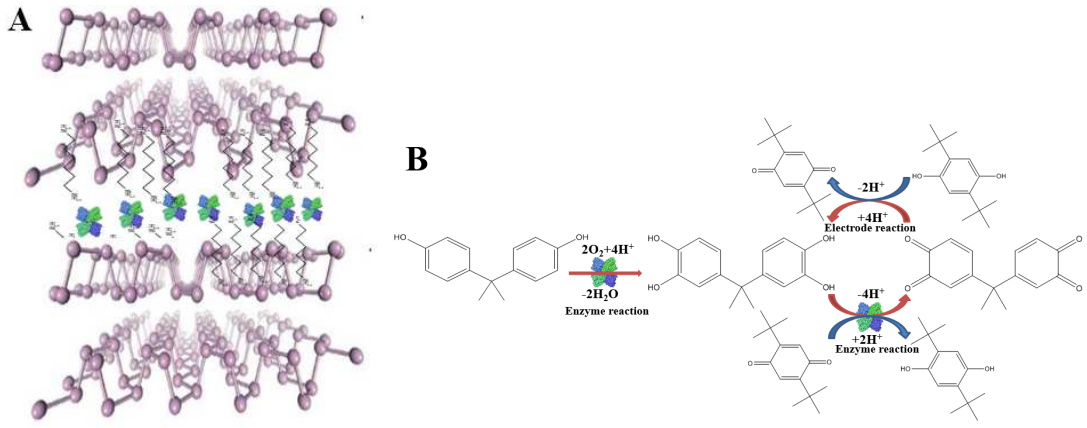

Scheme 2 (A). Schematic diagram of the tyrosinase immobilized on the HA/BP, and (B). The mechanism of detection of BPA with DTBQ as the electrolyte.

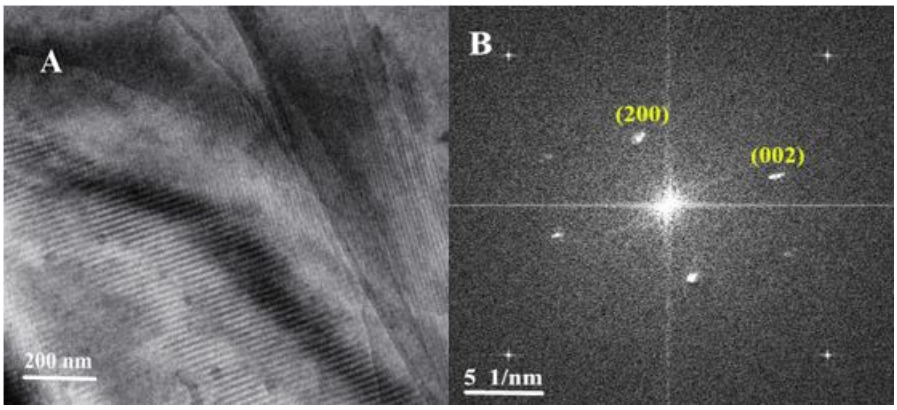

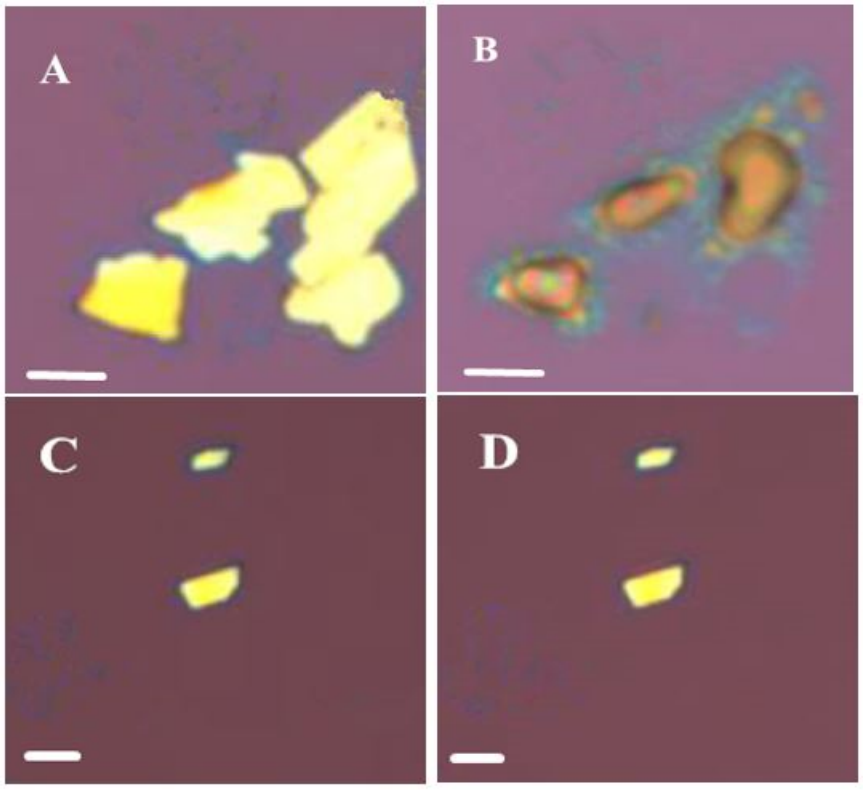
A
B
C
D

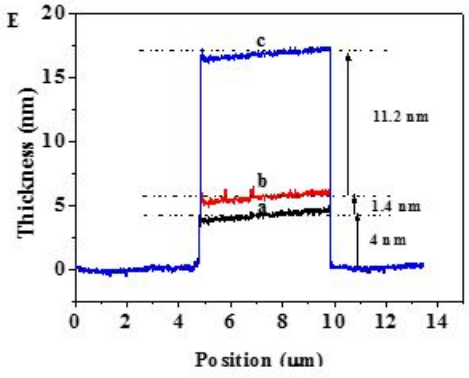
E
Thickness (nm)
Position (um)
c
b
a
11.2 nm
1.4 nm
4 nm

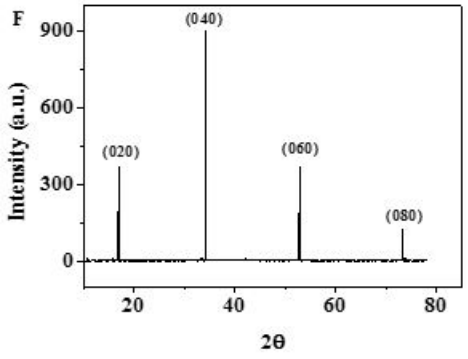
F
Intensity (a.u.)
2θ
(020)
(040)
(060)
(080)

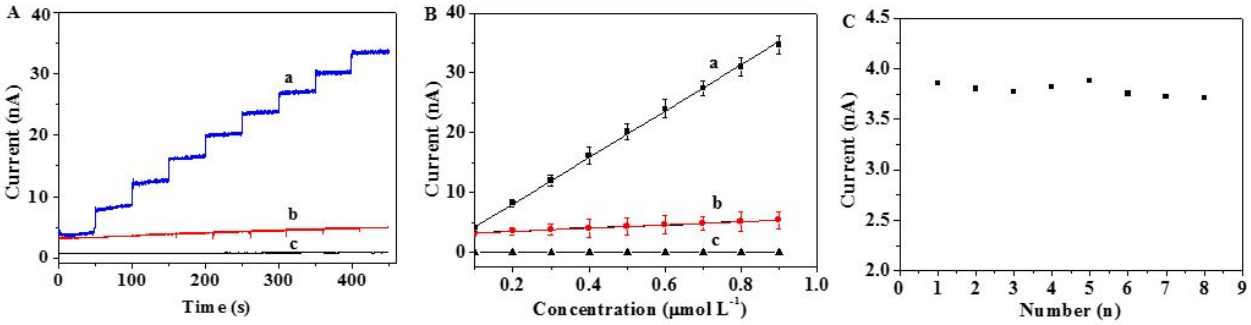

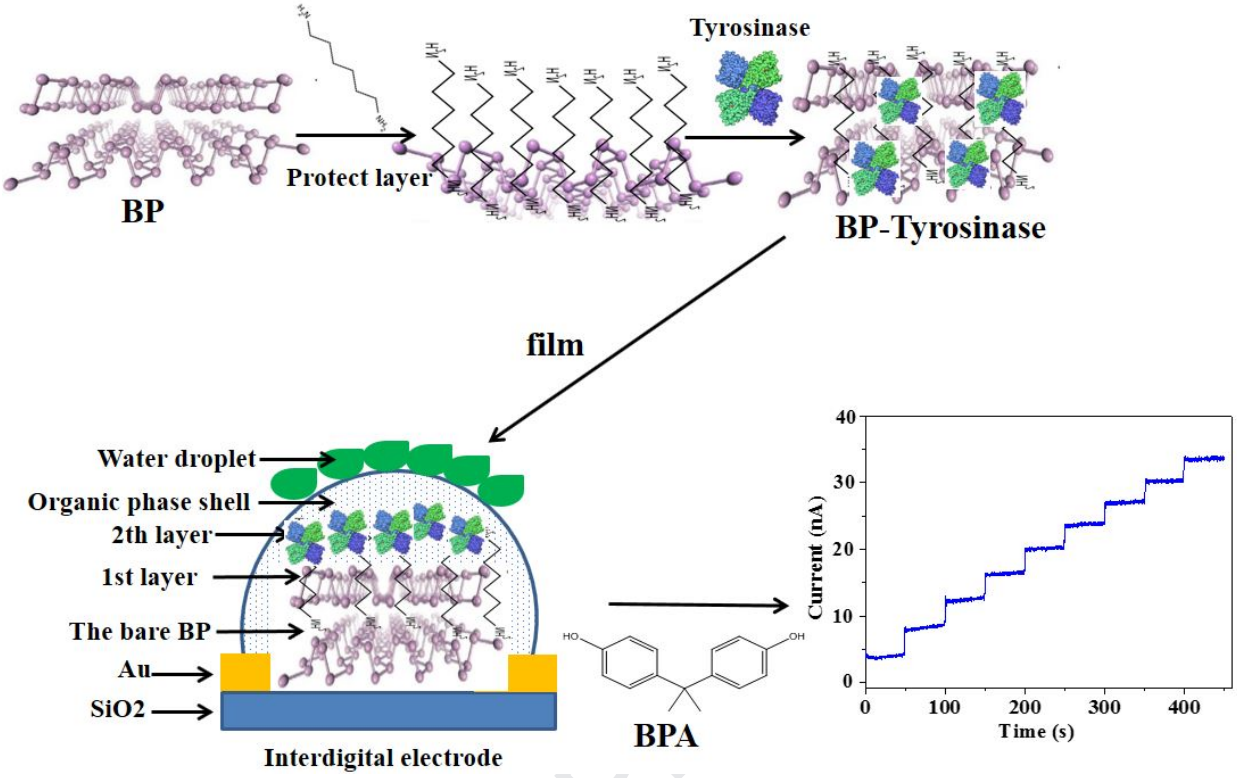

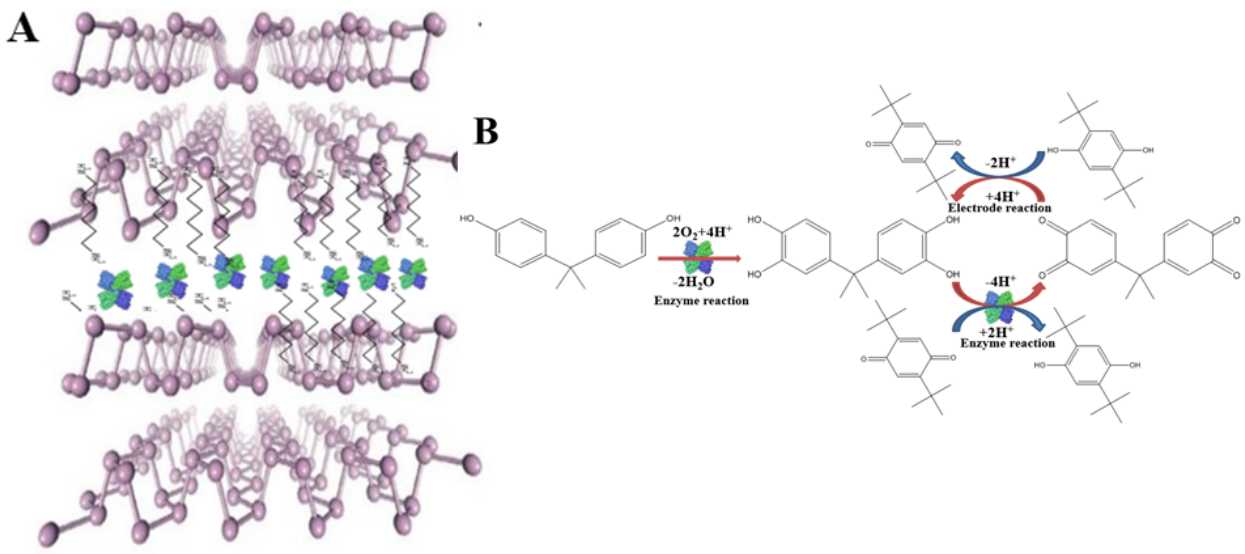

- The black phosphorene (BP) are exfoliated by ultrasonication in organic solvent.
- The stable BP is functionalized by hexamethylendiamine in organic solvent.
- 2,5-di-tert-butyl-1,4-benzoquinone is selected as new electrolyte.
- The detection limit (10 nmol L^{-1}) and the noise (0.025 nA) of this biosensor is the lowest among the reported biosensors.
- This biosensor retains over 65% of initial response signal after 180-day storage.

Declaration of interests

☒ The authors declare that they have no known competing financial interests or personal relationships that could have appeared to influence the work reported in this paper.

☐The authors declare the following financial interests/personal relationships which may be considered as potential competing interests: